



Proceedings of the Fifteenth International Conference on
Computational Structures Technology
Edited by: P. Iványi, J. Kruis and B.H.V. Topping
Civil-Comp Conferences, Volume 9, Paper 3.7
Civil-Comp Press, Edinburgh, United Kingdom, 2024
ISSN: 2753-3239, doi: 10.4203/ccc.9.3.7
©Civil-Comp Ltd, Edinburgh, UK, 2024

Topology Optimization of Lattice-Stiffener Hybrid Core for Composite Sandwich Panel

Y. Huang, T. Gao, L. Song, Y. Li, P. Fang and W. Zhang

**School of Mechanical Engineering, Northwestern Polytechnical
University
Xi'an, China**

Abstract

Hybrid core composite sandwich panels, as a typical load-bearing structure, have gained widespread recognition in various engineering fields due to their superior structural properties and outstanding multifunctional performances. However, the stiffeners and lattices in the structure will be staggered in the normal direction. Furthermore, the stiffeners in the in-plane direction are overly concentrated. Aiming at these problems, a multi-material topology optimization method with penetration constraint and maximum size constraint is proposed in this work. Lattices are equivalent to a virtual material by using energy-based homogenization method. To achieve the uniform distribution of stiffeners /lattices along the normal direction, the penetration constraint is proposed with local cylinder search region instead of traditional spherical search in the filtering process. Then the local porosity is introduced and local constraints are aggregated to the global one by p-mean function to achieve the precise size control of the stiffeners in the in-plane direction. The optimization model is efficiently solved utilizing a gradient-based optimization algorithm incorporating the sensitivity information. Finally, an engineering example is given to verify the validity and effectiveness of the proposed method.

Keywords: topology optimization, multi-material, hybrid core, stiffeners, lattices, composite sandwich panel, penetration constraint, maximum size constraint.

1 Introduction

Composite sandwich panels have been widely used in numerous fields such as aerospace, marine, and automotive industries attributable to their superior mechanical properties[1, 2]. A typical sandwich structure comprises two relatively thin high-strength composite panels and a thicker low-density core layer. Common lightweight core layers are constituted by cellular structures such as honeycomb, foam, and lattice, among others. The sandwich structure composed of foam and honeycomb has been widely applied[3]. With the deepening understanding of porous materials, the lattice structure is gradually showing broader prospects for application. In addition to mechanical advantages such as high specific stiffness and strength, its topological characteristics of open and interconnected single cells, along with highly customizable designs, are favored by researchers[4].

In recent years, the topology optimization method of lattice core sandwich structure has become a research hotspot. Huang et al. [5]proposed a topology optimization approach for designing the core unit cell in sandwich structures using the bi-directional evolutionary structural optimization (BESO) technique. Georges et al.[6] utilized homogenization and de-homogenization methods to optimize the strut diameter of the lattice core in sandwich panels. Zhang et al. [7]proposed a novel multiscale topology optimization method, enabling the design of high-performance gradient lattice core sandwich structures.

Hybrid core sandwich structures based on material hybridization reinforcement principles[8] provide greater design flexibility and enhance the overall performance of the structure than legacy lattice core sandwich structures. Sun et al. [9]proposed a biomimetic approach-based grid-honeycomb hybrid core design topology optimization method. Experimental results indicated that its mechanical performance surpasses the sum of honeycomb core specimens and grid core specimens. Yang et al. [1]proposed a lattice-foam hybrid core sandwich panel model, which enhances the absorption performance while meeting the load-bearing requirements. When it comes to engineering applications[10, 11], First perform a conventional topology optimization to achieve the layout result of the stiffeners, then fill the remaining space with lattice structures. It can be viewed that these aforementioned works are mainly based on intuitive bionics and empirical design. Differing from previous research, Li et al.[12] conducted the hybrid core sandwich structure design based on the concept of multi-material topology optimization, where stiffener and lattice materials are considered as separate material phases.

The design methodology based on the multi-material concept has successfully demonstrated its capability in creating solid-lattice hybrid structures[12, 13]. However, the current layout of lattice-stiffener hybrid core for composite sandwich panel exhibits the following problems: 1. The lattice and stiffener are mixed in the thickness direction. 2. The stiffeners are overly concentrated in the in-plane, which is not conducive to manufacturing processes. Therefore, it is an interesting research problem to control the size of the stiffeners while solving the layout of lattice-stiffener hybrid core for composite sandwich panel.

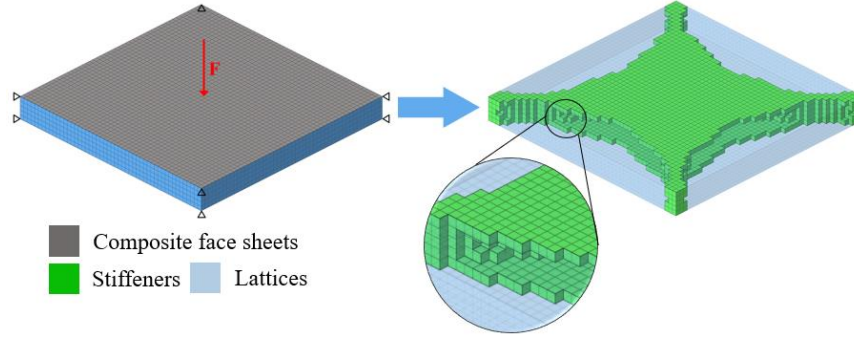


Figure 1: Problems in the layout of lattice-stiffener hybrid core for composite sandwich panel

In this work, a method is proposed for optimizing the layout of lattice-stiffener hybrid core in composite sandwich panels in the framework of the three-field approach of multi-material topology optimization. To ensure clear layout of the lattices and stiffeners, both penetration constraint and maximum size constraint are introduced and discussed in detail. A curved sandwich panel is designed and compared with the lattice core sandwich structures to reveal the effect of the proposed method.

2 Methods

A typical composite sandwich panel with lattice-stiffener hybrid core is shown in Figure 2. The structure consists composite face sheets and a lattice-stiffener hybrid core. In this study, composite face sheets were considered as non-designable domains, and the layout of the lattices and stiffeners in the core will be simultaneously designed. The general idea of the design method is outlined as follows: Firstly, the selected lattices are equivalent to the virtual homogeneous materials whose effective elastic matrixes are achieved by the energy-based homogenization method[12]. Secondly, the stiffeners are represented using solid material entities. Finally, the layout design of the lattice-stiffener hybrid core could be achieved by three-field approach of multi-material topology optimization.

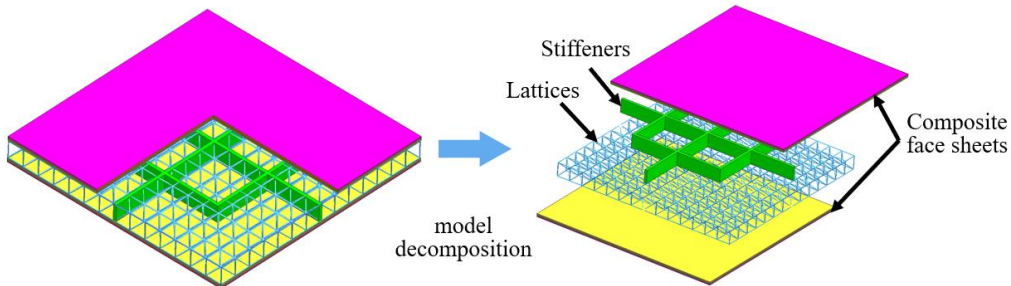


Figure 2: Schematic of composite sandwich panel with lattice-stiffener hybrid core

For the multi-material topology optimization problem, the so-called three-field are design variable field \mathbf{x} , filter variable field $\tilde{\mathbf{x}}$ and physical variable field $\bar{\mathbf{x}}$. Herein, \mathbf{x} denotes the set of design variables x_{ij} ($i = 1, \dots, n$; $j = 1, \dots, l$). n and l are the number of designable elements and candidate materials, respectively. In this work, $l = 2$ is the

number of hybrid cores. $j=1$ and $j=2$ represent the stiffeners and lattices, respectively.

To avoid the mesh dependency and checkerboard patterns, the density filter[14] is adopted here. The filtered variable \tilde{x}_{ij} can be calculated from design variable as

$$\tilde{x}_{ij} = \sum_{e \in N_i} W_{ie} v_e x_{ej} / \sum_{e \in N_i} W_{ie} v_e \quad (1)$$

with

$$N_i = \{e \mid d_{ie} \leq R\} \quad (2)$$

$$W_{ie} = \max(0, (1 - d_{ie} / R)) \quad (3)$$

where N_i represents the set of neighborhood elements e with the filter radius R to element i . The neighborhood is depicted as a sphere region in 3D problems, thus the center-to-center distance $d_{ie} = \sqrt{(x_i - x_e)^2 + (y_i - y_e)^2 + (z_i - z_e)^2}$. W_{ie} is the normalized weighting function, and v_e denotes the volume of element e .

The threshold projection[15], which serves as an efficient strategy, is widely employed in topology optimization to effectively suppress the emergence of gray transition regions. By using the smoothed Heaviside function suggested in[16], the physical variable is written as

$$\bar{x}_{ij} = H(x_{ij}^0) = \frac{\tanh(\beta\eta) + \tanh(\beta(x_{ij}^0 - \eta))}{\tanh(\beta\eta) + \tanh(\beta(1 - \eta))} \quad (4)$$

where β and η control the steepness and the threshold of the projection, respectively.

It is found that the three-field approach presented above leads to results in which the lattices and stiffeners are mixed in the thickness direction and the latter are overly concentrated in the in-plane direction. To achieve clear layout of the lattices and stiffeners, both penetration constraint and maximum size constraint are introduced, as shown in Figure 3. In the following sections, both constraints will be discussed in detail.

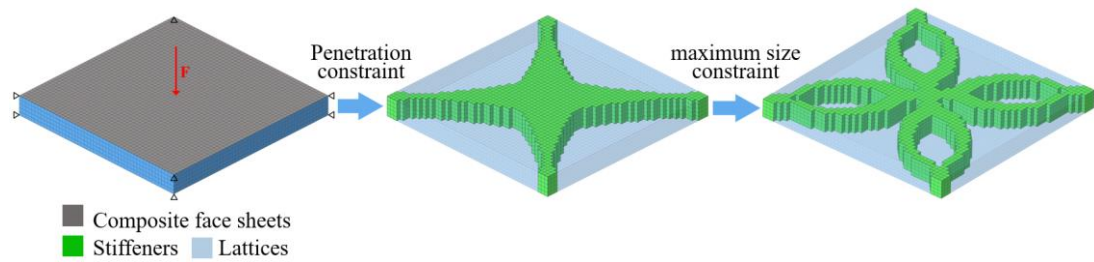


Figure 3: Schematic of layout design of hybrid core for composite sandwich panel

2.1 Penetration Constraint

As depicted in Figure 1, irregular mix of lattice and stiffeners is observed in the thickness direction, particularly at the marked location within the black circle. This phenomenon can be attributed to the characteristic low stress and strain levels

experienced by elements in proximity to the mid-surface regions. Nevertheless, the phenomenon would introduce complexity and higher costs to the manufacturing process. In order to eliminate this undesirable phenomenon, drawing inspiration from anisotropic filtering [17, 18], this study employs a cylindrical search region instead of the traditional spherical search region in the filtering process.

The schematic diagram of the cylindrical search region is shown in Figure 4. Herein, \bar{h} is the thickness of the panel. R is the radius of the cylinder, which corresponds to the filter radius mentioned above. h_{ie} is the projected distance in the axial direction from the central distance of element i and e , while d_{ie} is the projected distance in the radial direction from the central distance of element i and e . Based on the central coordinates of element $i(x_i, y_i, z_i)$ and element $e(x_e, y_e, z_e)$, the element neighborhood set N_i is revised as

$$N_i = \left\{ e \mid \begin{cases} d_{ie} = \left((x_i - x_e)^2 + (y_i - y_e)^2 \right)^{0.5} \leq R \\ h_{ie} = |z_i - z_e| \leq \bar{h} \end{cases} \right\} \quad (5)$$

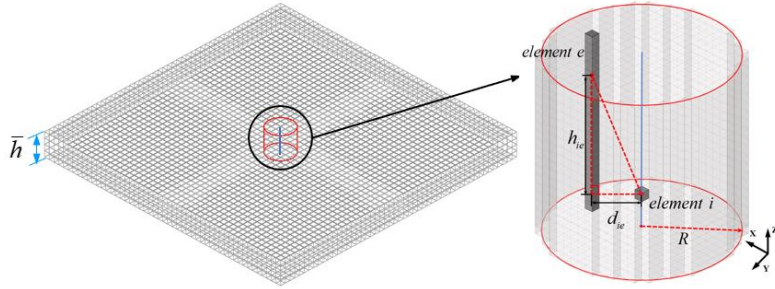


Figure 4: Cylindrical search region in flat sandwich panel

The fundamental principle involves the relaxation of the centroids distance from a three-dimensional (XYZ) space to a two-dimensional (XY) plane. This transformation ensures uniform weight distribution along the axial direction. It achieves the effect of penetration control, ensuring the same material along the normal direction of the sandwich panel.

The cylindrical search region can not only be applied to flat sandwich panels but also to curved sandwich panels with small curvature. As shown in Figure 5, the central axis line l_i of the cylinder passes through centroid of element i and is perpendicular to the sandwich panel. Its angle to the x -axis is θ . Thus, the central axis line l_i can be defined as

$$\begin{cases} y_i = \tan \theta \cdot x_i & \theta \in (0, \pi) \\ z = z_i \end{cases} \quad (6)$$

The distance from element e to l_i can be written as

$$d_{ie} = \sqrt{L^2 + (z_j - z_i)^2}, \quad L = |\tan \theta \cdot x_e - y_e| / \sqrt{1 + (\tan \theta)^2} \quad (7)$$

Then, the height of cylindrical search region is expressed as

$$h_{ie} = \sqrt{\Delta^2 - d_{ie}^2} \quad , \quad \Delta = \sqrt{(x_i - x_e)^2 + (y_i - y_e)^2 + (z_i - z_e)^2} \quad (8)$$

Finally, for curved sandwich panel, the element neighborhood set N_i is defined as

$$N_i = \{e \mid \{d_{ie} \leq R, h_{ie} \leq H\}\} \quad (9)$$

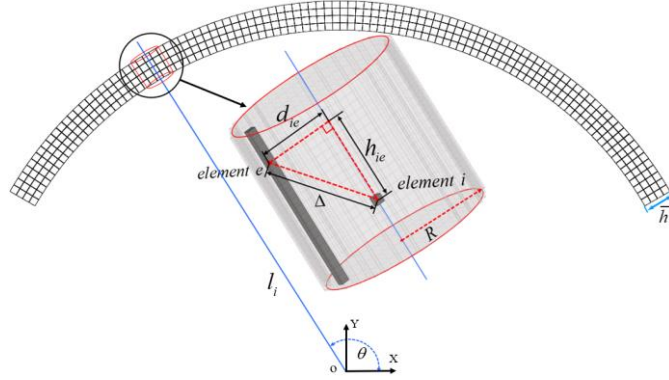


Figure 5: Cylindrical search region in curved sandwich panel

2.2 Maximum size constraint

To avoid the concentration of stiffeners limits in the in-plane direction and ensure thin stiffeners, the maximum size constraint is introduced. Based on pertinent research findings [18, 19], local maximum size constraints are typically defined by introducing porosity. The local constraints for stiffeners are defined as

$$g_i = \varepsilon_i - \frac{\sum_{k \in \Omega_i} v_k (1 - \bar{x}_{k1})^p}{\sum_{k \in \Omega_i} v_k} \leq 0 \quad (10)$$

where Ω_i is the maximum size region of element i and ε_i is the small positive lower limit of porosity for stiffeners. v_k is the volume of element k in the region Ω_i , p is the penalty factor, and \bar{x}_{k1} is the physical density for stiffeners. The most usual approach in literature is to define the region Ω_i as a sphere around the element i , as shown in Figure 6. R_{Max} represents the maximum size defined by the user.

However, the spherical search region is no longer suitable for sandwich structures, particularly when considering the relatively small dimensions in the thickness direction. Therefore, the cylindrical search region is introduced again to replace the spherical search region.

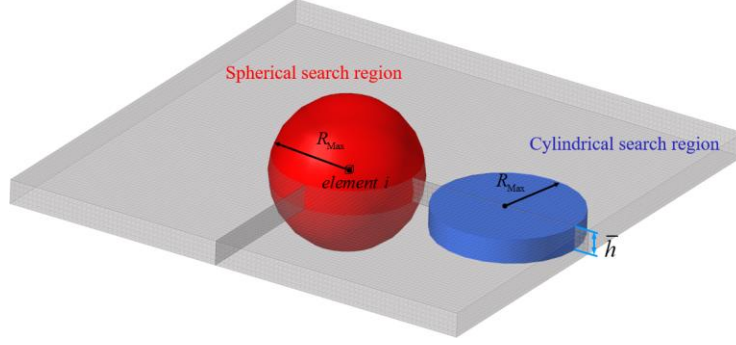


Figure 6: Spherical search region and cylindrical search region

The maximum size constraint presented above is inherently local and leads to a large number of constraints. In order to reduce the workload of the optimization algorithm, the local constraints are aggregated into a single one by using the p -mean function. Given that $g_i \in (\varepsilon, 1-\varepsilon)$, the definition of the aggregation function $s_i \in (0,1)$ is formulated in the following manner to be aggregated.

$$s_i = g_i + 1 - \varepsilon_i \quad (11)$$

Then, the p -mean aggregation function corresponds to

$$p_m = \left(\frac{1}{n_e} \sum_{i=1}^n (s_i)^{p_M} \right)^{1/p_M} \quad (12)$$

therein, n is the number of elements within the design domain and p_M is the exponent that controls the accuracy of the p -mean aggregation. According to Equation (11) and Equation(12), the global maximum size constraint can be expressed as

$$G_m = p_m - 1 + \varepsilon_i \leq 0 \quad (13)$$

2.3 Optimization formulation

The layout design optimization of the lattice-stiffener hybrid core for composite sandwich panel is solved by multi-material topology optimization, which can be expressed as the following mathematical programming problem. Thus the optimization formulation is stated as

$$\begin{aligned}
 &\text{find : } \mathbf{x} = \{x_{ij}\} \quad (i=1,2,\dots,n ; j=1,2,\dots,l) \\
 &\text{minimize : } C = \mathbf{U}^T \mathbf{K} \mathbf{U} \\
 &\text{subject to : } \mathbf{K} \mathbf{U} = \mathbf{F} \\
 &\quad \bar{x}_{ij} = H(\tilde{x}_{ij}) = H(W_i x_{ij}) \\
 &\quad M(\bar{x}_{ij}) \leq \bar{M} \\
 &\quad \sum_{j=1}^l \frac{V^{(j)}(\bar{x}_{ij})}{\bar{V}} = 1 \\
 &\quad G_m < 0 \\
 &\quad 0 < x_{\min} \leq x_{ij} \leq 1
 \end{aligned} \quad (14)$$

The optimization objective is structure compliance C . \mathbf{K} , \mathbf{U} and \mathbf{F} represent the global stiffness matrix, the nodal displacement vector, and the external load vector, respectively. M and \bar{M} denote the mass and its upper bound of all designable elements, respectively. $V^{(j)}$ denotes the volume usage of j th material. G_m is the maximum size constraint for stiffeners. A lower bound for the design variables x_{\min} (10^{-9}) is introduced to avoid the singularity of the structural stiffness matrix in the finite element analysis.

In finite element analysis, the element stiffness matrix could be written as

$$\mathbf{K}_i = \int_{V_i} \mathbf{B}_i^T \mathbf{D}_i \mathbf{B}_i dV \quad (15)$$

where \mathbf{B}_i and \mathbf{D}_i are, respectively, the strain-displacement matrix and the element constitutive matrix. Generally, the element constitutive matrix can be parameterized as a weighted sum of the constitutive matrices of the candidate materials.

$$\mathbf{D}_i = \sum_{j=1}^l w_{ij} \mathbf{D}^{(j)} \quad (16)$$

where $\mathbf{D}^{(j)}$ is the constitutive matrix of the j th candidate material, and w_{ij} is the weighting function of designable element i with material phase j . And the weighting functions are expressed as

$$w_{ij} = x_{ij}^p \prod_{\substack{\xi=1 \\ \xi \neq j}}^l (1 - x_{i\xi}^p) \quad (17)$$

where p represents the penalization power, usually chosen as $p=3$.

The volume usage of j th material $V^{(j)}$ can be calculated by the following equation

$$V^{(j)} = \sum_{i=1}^n \bar{x}_{ij} V_i \quad (18)$$

And also the mass of all designable elements is expressed as

$$M = \sum_{i=1}^n \sum_{j=1}^l \bar{x}_{ij} \rho^{(j)} V_i \quad (19)$$

2.4 Sensitivity analysis

Topology optimization problems are typically solved using gradient-based optimizers. Consequently, in this section, the first-order sensitivity information of the objective and constraint functions with respect to the design variables are derived.

Using the chain rule, the sensitivity of a certain scalar function f with respect to the design variables x_{ej} can be rewritten as

$$\frac{\partial f}{\partial x_{ej}} = \frac{\partial f}{\partial \bar{x}_{ij}} \frac{\partial \bar{x}_{ij}}{\partial x_{ej}} \quad (20)$$

where $\partial \bar{x}_{ij} / \partial x_{ej}$ can be easily exported from Equation(4)

$$\frac{\partial \bar{x}_{ij}}{\partial \mathcal{X}_{ij}} = \frac{\beta \left[1 - \tanh^2 \left(\beta (\mathcal{X}_{ij} - \eta) \right) \right]}{\tanh(\beta \eta) + \tanh(\beta (1 - \eta))} \quad (21)$$

Similarly, $\partial \mathcal{X}_{ij} / \partial x_{ej}$ is computed by Equation(1)

$$\frac{\partial \mathcal{X}_{ij}}{\partial x_{ej}} = \frac{W_{ie} v_e}{\sum_{e \in N_i} W_{ie} v_e} \quad (22)$$

The derivatives of the objective and constraint functions with respect to \bar{x}_{ij} are derived in detail as follows. It is worth noting that the sensitivity analysis of the penetration constraint is derived from Equation(22). The sensitivity analysis of the volume constraint is straightforward and therefore omitted here.

The sensitivity of the structural compliance with respect to physical densities \bar{x}_{ij} corresponds to

$$\frac{\partial C}{\partial \bar{x}_{ij}} = -\mathbf{U}^T \frac{\partial \mathbf{K}}{\partial \bar{x}_{ij}} \mathbf{U} \quad (23)$$

Evidently, $\partial \mathbf{K} / \partial \bar{x}_{ij}$ can be easily exported at the element level.

$$\frac{\partial \mathbf{K}}{\partial \bar{x}_{ij}} = \int_{V_i} \mathbf{B}_i^T \frac{\partial \mathbf{D}_i}{\partial \bar{x}_{ij}} \mathbf{B}_i dV = \sum_{\kappa=1}^l \left(\frac{\partial w_{i\kappa}}{\partial \bar{x}_{ij}} \mathbf{K}_i^{(\kappa)} \right) \quad (24)$$

with

$$\mathbf{K}_i^{(\kappa)} = \int_{V_i} \mathbf{B}_i^T \mathbf{D}^{(\kappa)} \mathbf{B}_i dV \quad (25)$$

The partial derivative of the weighting functions can be expressed as

$$\frac{\partial w_{i\kappa}}{\partial \bar{x}_{ij}} = \begin{cases} p \bar{x}_{ij}^{p-1} \prod_{\xi=1, \xi \neq j}^l (1 - \bar{x}_{i\xi}^p) & (\kappa = j) \\ -p \bar{x}_{ij}^{p-1} \prod_{\substack{\xi=1 \\ \xi \neq j, \xi \neq \kappa}}^l (1 - \bar{x}_{i\xi}^p) & (\kappa \neq j) \end{cases} \quad (26)$$

The sensitivity of the mass constraint is derived as

$$\frac{\partial M}{\partial \bar{x}_{ij}} = \rho^{(j)} V_i \quad (27)$$

The sensitivity of the global maximum size constraint is obtained by using the chain rule as follows

$$\frac{\partial G_m}{\partial \bar{x}_{ij}} = \frac{\partial G_m}{\partial p_m} \sum_{k \in \Omega_i} \left(\frac{\partial p_m}{\partial s_k} \frac{\partial s_k}{\partial g_k} \frac{\partial g_k}{\partial \bar{x}_{ij}} \right) \quad (28)$$

Evidently, $\partial G_m / \partial p_m = 1$ and $\partial S_k / \partial g_k = 1$. $\partial g_k / \partial \bar{x}_{ij}$ and $\partial p_m / \partial s_k$ hold as

$$\frac{\partial g_k}{\partial \bar{x}_{ij}} = \frac{p v_i (1 - \bar{x}_{ij})^{p-1}}{\sum_{k \in \Omega_i} v_k}, \quad \frac{\partial p_m}{\partial s_k} = \frac{1}{n_e} (p_m)^{1-p_m} (s_k)^{p_m-1} \quad (29)$$

Finally, the sensitivity of the global maximum size constraint yields

$$\frac{\partial G_m}{\partial \bar{x}_{ij}} = p v_i (1 - \bar{x}_{ij})^{p-1} \frac{(p_m)^{1-p_M}}{n_e} \sum_{k \in \Omega_i} \left(\frac{(s_k)^{p_M-1}}{\sum_{k \in \Omega_i} v_k} \right) \quad (30)$$

3 Results

In this section, a simplified aerospace curved sandwich panel with aerodynamic loads is tested to illustrate the effectiveness of the above-described optimization scheme. In the sandwich panels, composite face sheets and the core layer are discretized by using solid shell elements and solid elements, respectively. In this work, the core layer is discretized into five-layer finite elements. Herein, the anisotropic material carbon fiber reinforced epoxy resin (T300/BMP-316) and the isotropic material Aluminium alloy are available. Their properties are listed in Table 1.

Material	Elastic modulus [GPa]	Poisson's ratio [-]	Density [kg·m ⁻³]
T300/BMP-316	$E_{11}=123, E_{22}=E_{33}=8.4$	$\mu_{12}=\mu_{13}=0.32, \mu_{23}=0.3$	1560
Aluminium alloy	70	0.3	2700

Table 1: Material properties

The finite element model and geometric dimensions of an aerospace curved sandwich panel are shown in Figure 7. The panel structure encompasses a designable region, an inner and outer composite face sheet, and a long non-design domain. The inner and outer composite face sheets are made of unidirectional T300/BMP-316 with a nominal thickness of 0.125 mm. Two composite face sheets contain four prepreg plies stacked in [90/-45/45/0] and [0/45/-45/90] sequences, respectively. A uniform aerodynamic pressure of 1 MPa is applied to the upper face sheet and fixed constraints are imposed on the non-design domain. The designable domain should be filled with stiffeners and lattices, and its material is Aluminium alloy. According to the design requirements, the mass of the design domain must be less than 1.4 kg.

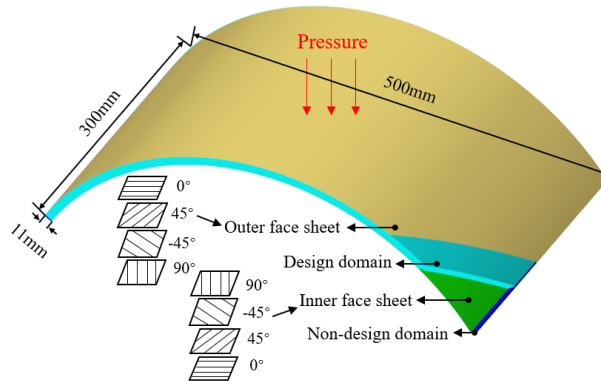


Figure 7: Finite element model and dimensions

In this paper, a body-center-cubic (BCC) microstructure is used as the lattice material cell, which has tensile and compressive resistance, shear capability, self-supporting advantages, and easy bonding with composite face sheets. The equivalent elastic matrix of lattice material can be obtained by the energy homogenization method. The properties of the BCC lattice unit cell are given in Table 2.

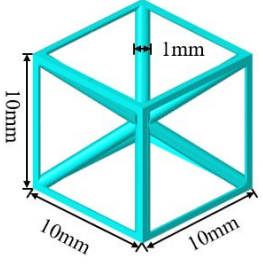
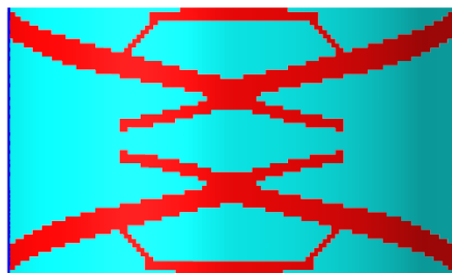
Lattice unit cell	Volume fraction	Equivalent elastic matrix [GPa]
	6.79%	$\begin{bmatrix} 1.098 & 0.483 & 0.483 & & & \\ 0.483 & 1.098 & 0.483 & & & \\ 0.483 & 0.483 & 1.098 & & & \\ & & & 0.456 & & \\ & & & & 0.456 & \\ & & & & & 0.456 \end{bmatrix}$

Table 2: The properties of BCC lattice

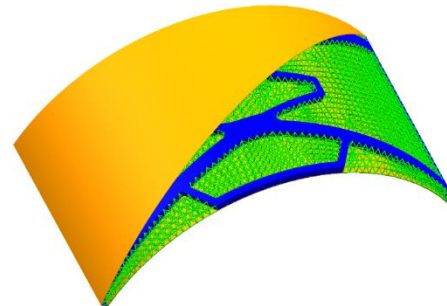
The filter radius $R_f = 1.5\text{mm}$, and maxsize radius $R_{\max} = 8\text{mm}$. The porosity for ribs is 0.05. The optimized configuration is shown in Figure 8(a). According to the obtained optimization configuration, the reconstructed panel structure is illustrated in Figure 8(b). The mass of lattice-stiffener hybrid core is 1.416 kg. It is worth noting that the reconstruction and optimized configurations are slightly different, primarily due to the consideration of manufacturability during the remoding process.

In order to verify the mechanical properties of the hybrid core composite sandwich panel, the lattice core composite sandwich panel with the same weight was reconstructed, as shown in Figure 9. Taking into account the practical manufacturing process of the lattice, its rod diameter is set at 1.8mm. Finally, the mass of lattice core is 1.463 kg.



■ Stiffeners ■ Lattices

(a) Optimized configuration



(b) Hybrid core composite sandwich panel

Figure 8: Optimized result and reconstruction

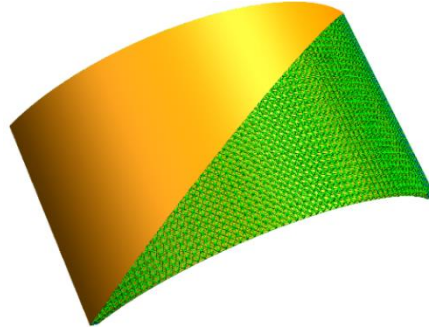


Figure 9: Lattice core composite sandwich panel

Static analysis and modal analysis were carried out on the hybrid core composite sandwich panel and the lattice core composite sandwich panel, and the results are shown in Table 3.

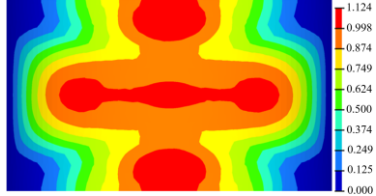
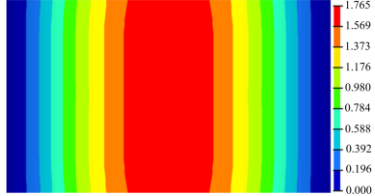
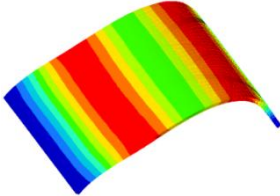
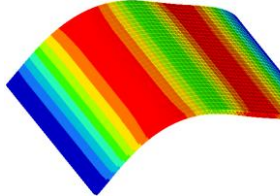
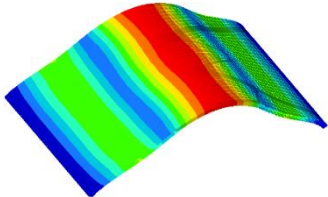
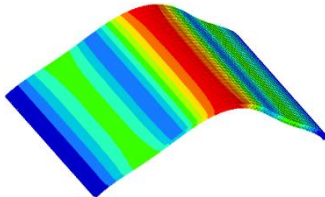
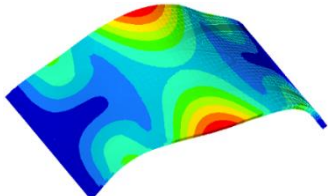
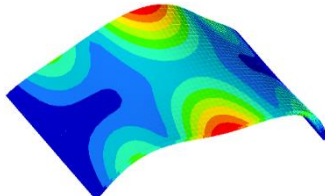
Model Index	hybrid core Composite sandwich panel	lattice core Composite sandwich panel
Core mass [kg]	1.416	1.463
Displacement [mm]	 $U_{\max} = 1.124$	 $U_{\max} = 1.765$
First natural frequency [Hz]	 $f_1 = 399.8$	 $f_1 = 347.3$
Second natural frequency [Hz]	 $f_2 = 749.8$	 $f_2 = 651.7$
Third natural frequency [Hz]	 $f_3 = 824.5$	 $f_3 = 671.5$

Table 3: Numerical analysis results of two composite sandwich panels

Based on the aforementioned comparison, the hybrid core composite sandwich panel demonstrates the greatest stiffness, with a maximum deformation reduction of 36.3% compared to the lattice core composite sandwich panel. In terms of dynamic performance, the first three modal shapes of both hybrid core sandwich panel and lattice core sandwich panel show similar characteristics. However, the former demonstrates significantly higher natural frequencies, suggesting superior structural rigidity and response. Therefore, the hybrid core composite sandwich panel has comprehensive performance advantages over the lattice core composite sandwich panel.

4 Conclusions and Contributions

To address the issues of dislocated distribution of stiffeners /lattices in their normal direction, as well as concentrated distribution of stiffeners within the plane, we introduce penetration constraint and maximum size constraint and obtain the hybrid core layout by three-field approach of multi-material topology optimization, which improves the manufacturability of the structure. The main conclusions are as follows:

(1) The penetration constraint is implemented by introducing cylindrical search instead of spherical search. This transformation ensures uniformity of weights along the normal direction, thereby achieving the uniform distribution of stiffeners /lattices.

(2) During the process of maximizing control for the sandwich panel, the cylindrical search is re-initiated, enabling precise control over the size of the stiffeners within the plane.

(3) The simulation results reveal that the hybrid core composite sandwich panel exhibits superior dynamic and static properties compared to the lattice core composite sandwich panel under the same mass constraint.

This paper introduces the penetration constraint and the maximum size constraint applicable to sandwich structures. However, further investigations are needed, such as the collaborative optimization of composite face sheets and hybrid core layout.

Acknowledgements

This work is supported by the National Key Research and Development Program of China (2022YFB4602001) and the National Natural Science Foundation of China (12172294).

References

- [1] L. Yang, H. Fan, J. Liu, Y. Ma, Q. Zheng, "Hybrid lattice-core sandwich composites designed for microwave absorption", *Materials & Design*, Vol.50, 863-871, 2013.
- [2] M. Alfounh, J. Ji, Q. Luo, "Optimal design of multi-cellular cores for sandwich panels under harmonic excitation", *Composite Structures*, Vol.248, 112507, 2020.
- [3] C. Qi, F. Jiang, S. Yang, "Advanced honeycomb designs for improving mechanical properties: A review", *Composites Part B: Engineering*, 227, 2021.

- [4] M.I. Chibinyani, T.C. Dzogbewu, M. Maringa, A. Muiruri, "Lattice Structures Built with Different Polygon Hollow Shapes: A Review on Their Analytical Modelling and Engineering Applications", *Applied Sciences*, Vol.14, 1582, 2024.
- [5] X. Huang, Y.M. Xie, "Optimal design of periodic structures using evolutionary topology optimization", *Structural and Multidisciplinary Optimization*, Vol.36, 597-606, 2008.
- [6] H. Georges, C. Mittelstedt, W. Becker, "RVE-based grading of truss lattice cores in sandwich panels", *Archive of Applied Mechanics*, 93, 3189-3203, 2023.
- [7] Y. Zhang, M. Xiao, X. Zhang, L. Gao, "Topological design of sandwich structures with graded cellular cores by multiscale optimization", *Computer Methods in Applied Mechanics & Engineering*, Vol.361, 112749, 2020.
- [8] M.F. Ashby, Bréchet, Y.J.M. View Correspondence, "Designing hybrid materials(Article)", *Acta Materialia*, Vol.51, 5801-5821, 2003.
- [9] Z. Sun, D. Li, W. Zhang, S. Shi, X. Guo, "Topological optimization of biomimetic sandwich structures with hybrid core and CFRP face sheets", *Composites Science and Technology*, 142, 79-90, 2017.
- [10] G. Dong, Y. Tang, D. Li, Y.F. Zhao, "Design and optimization of solid lattice hybrid structures fabricated by additive manufacturing", *Additive Manufacturing*, 33, 2020.
- [11] J.-E. Kim, K. Park, "Multiscale Topology Optimization Combining Density-Based Optimization and Lattice Enhancement for Additive Manufacturing", *International Journal of Precision Engineering and Manufacturing-Green Technology*, 8, 1197-1208, 2020.
- [12] Y. Li, T. Gao, Q. Zhou, P. Chen, D. Yin, W. Zhang, "Layout design of thin-walled structures with lattices and stiffeners using multi-material topology optimization", *Chinese Journal of Aeronautics*, 2022.
- [13] Y. Li, W. Qiu, Z. Liu, Y. Liu, L. Xia, "A multi-material topology optimization approach to hybrid material structures with gradient lattices", *Computer Methods in Applied Mechanics and Engineering*, 425, 2024.
- [14] E. Andreassen, A. Clausen, M. Schevenels, B.S. Lazarov, O. Sigmund, "Efficient topology optimization in MATLAB using 88 lines of code", *Structural and Multidisciplinary Optimization*, 43, 1-16, 2010.
- [15] J.K. Guest, J.H. Prévost, T. Belytschko, "Achieving minimum length scale in topology optimization using nodal design variables and projection functions", *International Journal for Numerical Methods in Engineering*, 61, 238-254, 2004.
- [16] F. Wang, B.S. Lazarov, O. Sigmund, "On projection methods, convergence and robust formulations in topology optimization", *Structural and Multidisciplinary Optimization*, 43, 767-784, 2010.
- [17] L. Song, T. Gao, J. Wang, W. Zhang, "Directional maximum length scale control in density-based topology optimization", *Computers & Structures*, 292, 2024.
- [18] B. Wang, Y. Zhou, K. Tian, G. Wang, "Novel implementation of extrusion constraint in topology optimization by Helmholtz-type anisotropic filter", *Structural and Multidisciplinary Optimization*, 62, 2091-2100, 2020.